Materials Advances

ROYAL SOCIETY OF CHEMISTRY

PAPER

View Article Online
View Journal | View Issue

Cite this: *Mater. Adv.*, 2024, 5, 695

Eco-friendly one-shot approach for producing a functionalized nano-torrefied biomass: a new application of ball milling technology†

Aida Kiani,[a] Elena Lamberti,[b] Gianluca Viscusi,[b] Paola Giudicianni,[c] Corinna Maria Grottola,[c] Raffaele Ragucci,[b] Giuliana Gorrasi[b] and Maria Rosaria Acocella *[a]

A green and sustainable functionalization of the solid residue from populous nigra treated at low temperature (T = 285 °C) with a mechanochemical approach is reported here. The reaction is performed in the presence of dodecyltriphenyl phosphonium bromide to produce a new filler with antimicrobial activity. By selecting the right pyrolysis temperature, oxygen functionalities can be obtained on the carbon surface, avoiding the additional oxidation step to further modify the carbon material. In a one-step procedure, the filler is nanometrically reduced and is properly functionalized *via* cation exchange in a short time (*i.e.* 30 minutes) under dry conditions, providing a salt uptake of about 15 wt%. The new adduct exhibits high dispersibility on cotton fabrics and shows photocatalytic activity which confirms the capability of the manufacture to inhibit the organic contaminants' growth.

Received 4th October 2023,
Accepted 2nd December 2023

DOI: 10.1039/d3ma00804e

rsc.li/materials-advances

1 Introduction

Biochar is a carbon-rich material produced by pyrolysis of biomass in an oxygen-limited or inert atmosphere.[1] Among the thermochemical biomasses treatments, pyrolysis offers both great flexibility and a relatively easy way to control the yield and characteristics of the products. Pyrolysis temperature and heating rate are the main variables affecting the biochar yield and properties in terms of surface area, degree of carbonization, and elemental composition. In addition, the intrinsic composition of the feedstock determines the quality of the produced biochar.[2,3] Although the types of biomass vary greatly in composition, most of lignocellulosic biomasses contain organic components and inorganic elements that follow different pathways of decomposition and devolatilization during the thermal process, and their interactions determine different biochar yields and properties. At temperatures lower than 300 °C pyrolysis is generally referred to as torrefaction, and the solid residue is appropriately defined as torrefied biomass.[4,5] During the torrefaction, the solid residue is the result of dehydration and depolymerization reactions of hemicellulose resulting in increased carbon and reduced oxygen content, mostly C and O contents are in the range of 70–80 wt% and 10–30 wt%, respectively.[6,7] As the temperature increases, under pyrolysis regime, the H/C and O/C atomic ratio also decreases, indicating a release of hydrogen and oxygen-containing groups from the biochar.[8] As a result, lower H/C ratios correspond to less functional groups and more aromatic structure of the biochar. Hence, the functionalities and the surface chemistry of biochar are affected by both the degree of carbonization and the removal of acid groups.[9] The functional groups on the surface of biochar are hydrophobic, hydrophilic, acid, or basic. Within the last two categories, carboxyl groups are the strongest acids exhibited on the biochar surfaces, whereas phenols and carbonyls are the less acid groups.[10] Consequently, the pH of biochar increases from mild acid to basic values.[11]

The most significant physical changes during pyrolysis on biochar production occur at higher temperatures in terms of well-developed porosity, especially in the temperature range 350–600 °C.[12]

Porosity, a key property for biochar applications that involve interaction with a fluid stream, is correlated to the specific surface area usually measured by BET analysis.[13] Great development of the specific surface area can be achieved in the case of the biochar produced under steam-assisted pyrolysis conditions. For example, biochar with BET equal to 380 $m^2\ g^{-1}$ is produced from steam-assisted slow pyrolysis of eucalyptus at

[a] *Department of Chemistry and Biology, University of Salerno, via Giovanni Paolo II, 132, Fisciano (SA), 84084, Italy. E-mail: macocella@unisa.it*
[b] *Department of Industrial Engineering, University of Salerno, via Giovanni Paolo II, 132, Fisciano (SA), 84084, Italy*
[c] *Institute of Sciences and Technologies for Sustainable Energy and Mobility (STEMS) of the National Research Council (CNR), Naples, Italy*

† Electronic supplementary information (ESI) available. See DOI: https://doi.org/10.1039/d3ma00804e

700 °C.[2] In contrast, the porosity is significantly lower for biochar produced in an inert atmosphere.[14]

Each biochar chemical–physical property determines its applicability in different fields. Recently, biochar has received growing attention in several application fields, such as removing pollutants,[3] remediating soil,[15] and reducing greenhouse gas emissions but also in other novel applications: material in asphalt road construction,[16] filler in carbon nanotubes, NH_3 adsorbing cover of the manure storage tanks[17] and catalyst for biogas production.[18] As well as pyrolysis, other physical (steam, plasma, *etc.*) and chemical treatments (acid or alkaline pretreatment, oxidation, nitrogenation, *etc.*) also play a crucial role in better affecting and possibly improving their properties. It is possible to positively modify the biochar surface by introducing oxygen, nitrogen, and sulfur functionalities in order to enhance possible interactions with such a substrate and its performance for specific applications.[19]

Lately, considerable attention has been paid to this material as a filler for polymer matrices to provide polymer composites with enhanced electrical and mechanical properties,[20,21] finding many applications in the composite/polymer sector. The low cost and the eco-friendly nature of this carbon-based material could allow biochar to be a possible leader among carbon materials in composites.

In order to enhance the properties of the polymer, it's important to achieve good dispersibility of the filler. This can be obtained by using nanometric particle size and ensuring physical interactions between the filler and the polymer matrix. Because of the heterogeneous shape of biochar particles, depending on the feedstock properties and pyrolysis conditions, it is often necessary to grind the powder to reach the nanometer scale.[22]

On the other hand, it is possible to enhance the physical interactions between the filler and polymer matrices by modifying the carbon surface. This can be achieved by introducing new oxygenated functionalities by an oxidation step.[23–26] It is possible to avoid this additional step by using biochars produced by pyrolysis at low temperatures,[8] which provides oxygen functionalities to the char so that it can be further modified *via* ionically or covalent approaches and tailor its properties to the particular application. An easy chemical modification on carbon surface was recently reported by using an eco-friendly procedure, where the ability of carbon black to form an ionic bond with quaternary phosphonium salt using a dry planetary ball milling was investigated.[27]

The reaction takes place in 30 minutes without solvent and any additional reagent, through the breaking or building of chemical bonds by applying both impact and shear forces to particles that collide with the milling balls. First elastic forces and then irreversible plastic deformations generate new surfaces of the reactant easier to contact and react.

By choosing the right conditions such as the nature and dimension of the balls, the weight ratio of the balls/sample, rotation rate, milling time, and temperature, it is possible to reach the best ball milling performances. This new mechanochemical approach has shown to be promising because not only avoids solvents but also offers the opportunities for milder reaction conditions, ensuring energy efficiency and reduced environmental impact. Based on this previous research, we decided to investigate the ability of biochar to be chemically modified by using a mechanochemical procedure, introducing specific molecules on the carbon surface to modulate the polarity and the properties of the final composites.

Dodecyl triphenyl phosphonium bromide (DTPPBr) was chosen as a reference molecule because of the well-documented antimicrobial ability of quaternary phosphonium salt (QPS). In fact, it has been reported that with respect to using QPS as raw material in polymer matrices, an enhanced antimicrobial activity can be obtained when it is intercalated in organic clays[28] and graphite systems.[29] In particular, graphite intercalated compounds containing phosphonium salts showed significant antimicrobial activity against *E. coli* and *S. aureus* when compared to QPS simple mixed.

Recently, magnetic biochar/quaternary phosphonium salt composites (MBQ) have been reported with effective antimicrobial activities using the precipitation of iron oxide on biochar followed by ion exchange with quaternary phosphonium salt.[30] The MBQ proved to be an effective antimicrobial agent against Gram-negative bacteria *Escherichia coli* and Gram-positive bacteria *Staphylococcus aureus*, by exploiting the controllable release of QPS.

An alternative route to the introduction of metals is the chemical functionalization of QPS directly on the biochar surface. To this aim, in this study, the torrefied biomass and biochar from *Populous nigra* treated at low temperature (T = 285 °C) and high temperature (450 °C), and slow heating rate (10 °C min^{-1}) in an inert environment (N_2 = 12 slm), are characterized and tailored for application as filler. Only the material produced at low temperature is shown for the first time to ionically bond DTPPBr with a mechanochemical approach without a previous oxidation step. The resulting chemical-modified carbon filler has potential application as an antimicrobial material.

2 Experimental

2.1 Materials

Torrefied biomass and biochar derived from *Populus nigra* were produced in a fixed-bed reactor with a flexible configuration that allows to tune the main torrefaction and pyrolysis parameters. The experiments were conducted at a constant flow of nitrogen (N_2 = 12 slm) under slow heating, conditions (10 °C min^{-1}) up to the final temperature of 285 °C and 450 °C. The torrefied biomass and the biochar samples were labeled B1 and B2 respectively. Dodecyl triphenyl phosphonium bromide (DTPPBr), a quaternary phosphonium salt (QPS), with a purity of 98%, and resazurin were purchased from Sigma-Aldrich.

2.2 Feedstock and solid residue characterization

The biomass *Populus nigra* (P), and the corresponding solid residues after the thermal treatment (B1 and B2), were

characterized through proximate analysis using TGA701 LECO using ASTM E870 procedure. Additional TGA analyses for B1 and B2 were performed using Q500 TA Instruments from 10 to 800 °C at a heating rate of 10 °C, under nitrogen. Ultimate analysis was performed with an elemental analyzer CHN 2000 LECO analyzer, using EDTA as standard based on CEN/TS 15104. The oxygen was obtained by difference considering the measured C, H, N, and ash content calculated on a dry basis (db). The content of inorganic species was determined by dissolving the samples *via* microwave-assisted acid digestion based on US-EPA Methods 3051 and 3052. A representative sample (200 mg) of biomass was dissolved in 10 ml 65% nitric acid and 1.5 ml H_2O_2. The vessel was sealed and heated in the microwave unit at 140 °C for 10 min, then 180 °C for 30 min (maximum power 1000 W). After cooling the digested samples were analyzed by ICP/MS. The detection limit for all the heavy metals in the biomass is 0.1 mg kg^{-1}. Biomass, torrefied biomass, and biochar pH were evaluated by measuring with a digital pH meter (827 pH LAB, Metrohm) in deionized water using a 1 : 20 wt/wt ratio following the ASTM D4972-13 standard procedure, whereas the pH_{pzc} was determined following the procedure reported in Mahmood *et al.* (2011).[31] The porosity was obtained using an Autosorb-1 (Quantachrome) instrument with N_2 at −196 °C as the adsorbate gas. Before analysis, the samples were degassed at 200 °C for 6 h under vacuum conditions. The surface area was evaluated using the Brunauer–Emmett–Teller equation (BET). Three replicates were conducted for all the analysis and characterization.

2.3 Preparation of B1/DTTP and B2/DTPP compounds by ball milling

The ball-milling experiments were conducted using the planetary ball mill Pulverisette 7 Premium manufactured by Fritsch GmbH in Germany, operating at room temperature. The specific milling parameters employed for the experiments are outlined in Table 1. To carry out the procedures, an 80 ml silicon nitride jar was utilized, along with silicon nitride balls measuring 10 mm in diameter. The rotational frequency of the mill was set at 300 rpm, and the milling duration was fixed at 30 minutes. The samples were denoted as B1/DTPP with weight ratios of 1/0.5, 1/1, 1/2, and 1/3. The temperature inside the milling jar was continuously monitored using the Easy-GTM system from Fritsch GmbH. During the 30 minute milling process, the temperature gradually rose to 32 °C from the initial room temperature and remained stable throughout due to the milling procedure. The same methodology was applied to B2/DTPP with a weight ratio of 1/2.

3 Results and discussion

The solid residue from *Populous nigra* treated at low and high temperatures and slow heating rate (10 °C min^{-1}) in an inert environment (N_2 = 12 slm), was used in this study. The raw materials were fully characterized by elemental analysis (EA), FTIR, ICP, WAXD, SEM/EDX, and BET. The final temperature of the process had a crucial role in determining the solid yield and the characteristics of the torrefied biomass and biochar. At low temperature, namely, at 285 °C, the solid residue still preserves the biomass structure with a limited porosity, providing a yield of 67.5% of B1. (Table 1). Besides a reduced porosity, also the pH had a value typical of biomass. This result is in agreement with the hemicellulose decomposition that at 285 °C is already concluded, where most of the oxygenated compounds are still present in the torrefied biomass.

As expected, as the temperature increased up to 450 °C, a lower biochar yield of 32.5% was obtained. The carbon content increased with the pyrolysis temperature as well as the fixed carbon whereas the opposite trend occurred for the volatiles. A great amount of volatile matter was released at higher temperature resulting in sample B2 with 27.51 wt% of volatiles (Table 1).

As for ash, the content increases with temperature. The amount and composition of ash varies with the type of raw biomass. In the case of Poplar, most of the metals are alkali and alkaline earth metals, as reported in Table 2.

To thoroughly evaluate the chemical nature of the functional groups after low and high-temperature pyrolysis, infrared spectra were acquired on samples B1 and B2. As shown in Fig. 1, significant differences emerge from the comparison between B1 and B2, mainly regarding the 3800–3000 cm^{-1} region related to the OH group, where the OH stretching band is clearly evident for B1 and completely absent for B2. Moreover, the bands at 2922 and 2843 cm^{-1} are assigned to CH_2 stretching that completely disappears at higher pyrolysis temperatures. The broad band at 1705 cm^{-1} is compatible with the presence of unsaturated ketones and lactones on the surface, while the 1610 cm^{-1} band is associated with C═C stretching. Most interestingly, the region between 1550–1000 cm^{-1} shows many defined vibration peaks due to the persistence of lignin and cellulose structure for the low pyrolysis temperature. In particular, the peak at 1511 cm^{-1} represents the C═C vibration of lignin,[32] the 1463 cm^{-1} vibration is assigned to CH_2 bending, while the bands at 1422 and 1318 cm^{-1} are related to the bending of alcohol and phenol, respectively. Additionally, the vibrations in the region 1160–1027 related to C–O of primary

Table 1 Characterization of biomass (P) and corresponding solid residue (B1, B2)

	Yield	C	H	N	O	Fixed carbon	Volatiles	Ash			BET
Samples	wt%	wt% daf				wt% db			pH	pHpzc	$m^2\ g^{-1}$
Biomass	—	48.67	5.91	0.18	45.24	16.6	79.9	3.5	—	—	—
B1	67.5	58.43	5.17	0.34	36.06	30.54	64.32	5.14	7.3	7.22	1.6
B2	32.2	78.29	2.85	0.61	18.25	61.52	27.51	10.96	9.8	8.2	60

Table 2 ICP-MS analysis of biomass (P) and corresponding solid residue (B1, B2)

		Biomass	e^a (%)	BP-285 °C	e^a (%)	BP-450 °C	e^a (%)
Na	mg kg^{-1}	175	7	223	22	326	12
Mg		670	7	787	1	1627	15
Al		315	0	450	13	654	3
K		2511	16	3972	0	8397	21
Ca		11 000	8	13 435	10	27 330	9
Fe		790	1	1175	1	1785	17

[a] Percentage error is given in brackets.

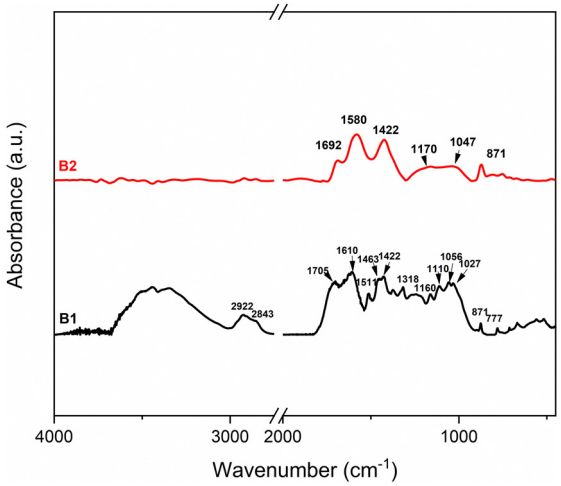

Fig. 1 FTIR of B1 and B2.

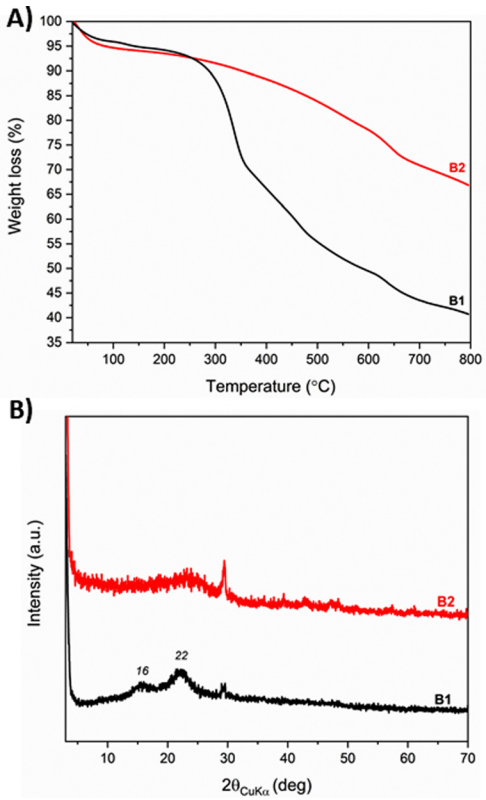

Fig. 2 TGA (A) and X-ray diffraction pattern (B) of B1 and B2.

and secondary alcohols and 1027 to the ether, are pronounced. Conversely, the FTIR for B2 shows broad bands at 1692, 1580, and 1422 cm^{-1} due to the presence of the carbonyl group, C=C vibration, and CH_2 bending, respectively. The disappearance of some vibrations and the broadening of bands are due to the structural modification that comes from higher temperature treatment and indicate a decrease in the nonpolar group contents.

The reduction of the oxygen content in B2 was further confirmed by the TGA analysis (Fig. 2(A)) under nitrogen flow, which shows a significant variation in the residue above 350 °C reaching only 34% of mass loss at 800 °C.

XRD diffraction pattern of B1, shown in Fig. 2(B), displays two broad peaks at the 2θ values around 16° and 22° relative to the crystalline region of cellulose in wood.[33] Increasing the pyrolysis temperature at 450 °C to provide B2, the crystalline cellulose is destroyed giving a broad reflection centered roughly on 23°.

Due to the significant presence of oxygen functionalities, mainly regarding the hydroxyl ones, B1 was chosen as a representative material to evaluate the possible ionic functionalization by using ball milling.

In a previous paper, the possibility of realizing new ionic compounds by using the mechanochemical approach was already reported for oxidized carbon black with a quaternary phosphonium salt, particularly with tetraphenyl phosphonium bromide. Nevertheless, the requirement to introduce the right functional groups, specifically carboxyl groups, limited the application to preventive oxidations of carbon materials. In particular, harsh conditions like those required from the Hummers oxidation were needed to provide the carboxyl functionalities essential for the cation exchange.[27]

Conversely, in the presence of a starting material such as B1, the extensive presence of hydroxyl groups suitable for cation exchange, could avoid the additional step of oxidation providing a completely green functionalization. Then, to verify the ability of B1 to be ionically functionalized by using the mechanochemical approach, the first reaction was performed in the conditions already optimized for oxidized carbon black.[27]

In a silicon nitride jar of 80 ml, the two reagents with a relative weight ratio between B1 and DTPPBr of 1 to 1 were mixed and milled at 300 rpm.

After 30 minutes of reaction performed on 150 mg of the mixture, the powder was collected, extensively washed with deionized water to remove the excess residue salt, and finally dried, providing the adduct named B1/DTPP in 92% mass yield.

The FTIR and X-ray analyses are shown in Fig. 3. FTIR (Fig. 3A(c)) of B1/DTPP shows the peaks at 503, 537, 686, 722, 754, 1110, and 1439, cm^{-1} related to DTPP. The X-ray diffraction pattern of B1/DTPP (Fig. 3B(c)), evidences that the crystalline cellulose phase is almost destroyed possibly due to the action of milling, providing a broad reflection centered around 23 °C. Additionally, it is also clear from the complete loss of

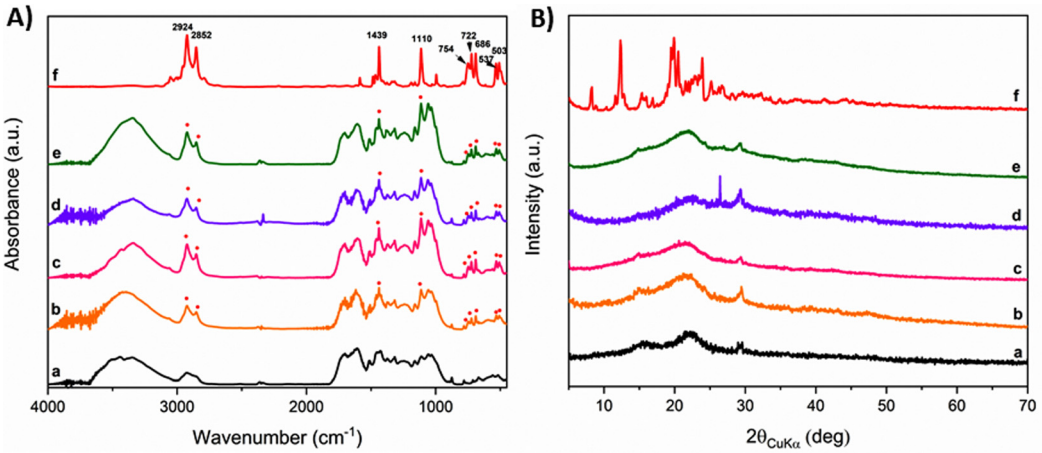

Fig. 3 FTIR (A) and WAXD (B) of B1 (a), B1/DTPP in a weight ratio of 1/0.5 (b), 1/1 (c), 1/2 (d) 1/3 (d) and DTPPBr (f).

DTPP crystallinity that an adduct is formed and that no residual salt is present on the powder surface.

To evaluate the DTPP uptake after the reaction, the B1/DTPP was analyzed by SEM/EDX providing interesting information about the particle size (Fig. 4) and elements distribution on the torrefied biomass surface. (Fig. 5).

As a result of ball milling action, the particle size is significantly reduced reaching the nanometric scale (Fig. 4f). The mean radii distribution is reported as inset showing that nanometric sized aggregates can be formed (up to 700 nm) with bigger aggregates which can reach micrometric size. The functionalization takes place providing a change in P weight % from 0.82 to 1.41 after the reaction, which corresponds to a DTPP uptake of 8.2 wt%. EDX analysis was carried out on the specimens and the atomic distributions of the characteristic elements are reported in Fig. 5.

In order to improve the DTPP uptake, additional experiments were performed changing the relative ratio between B1 and DTPP from 1/0.5 to 1/3, decreasing and increasing the DTPP salt, respectively. As reported in Fig. 3A, for B1/DTPP weight ratio of 1 to 0.5, a reduced functionalization occurs as evident from the less intense DTPP peaks in the B1/DTPP adduct (Fig. 3A(b)). Conversely, for a weight ratio of 1 to 2 and 1 to 3, no sensible differences can be detected, resulting in apparent similar DTPP uptake (Fig. 3A(d) and (e)).

Considering the initial amount of P present on the biochar surface, as the amount of DTPP increases in the reagent mixture, so does the amount of P in B1/DTPP. Specifically, as reported in Fig. 5, for B1/DTPP weight ratio of 1 to 0.5 a change in P weight % from 0.82 to 1.29 was detected which corresponds to 6.6 wt% uptake while for a weight ratio of 1 to 2, the P

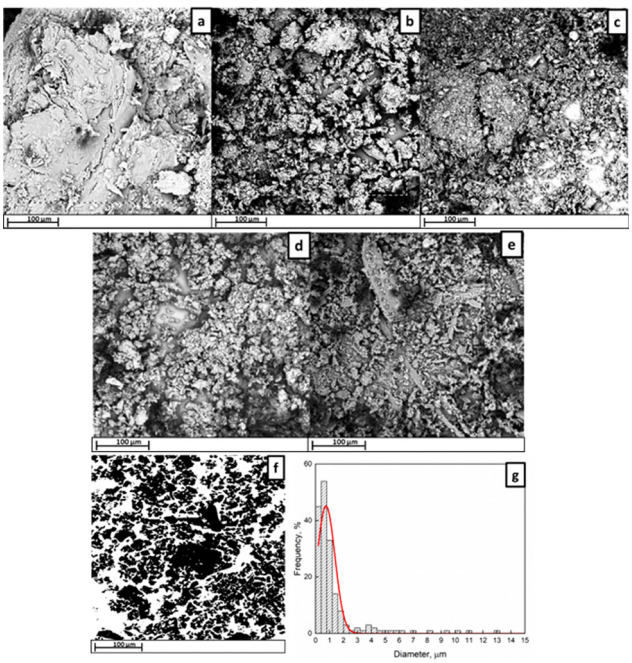

Fig. 4 SEM/EDX images of different B1/DTPP samples: (a) starting B1, (b) B1/DTPP prepared in ratio 1 to 0.5, (c) B1/DTPP prepared in ratio 1 to 1, (d) B1/DTPP prepared in ratio 1 to 2, (e) B1/DTPP prepared in ratio 1 to 3, (f) sample image analysis of B1/DTPP 1 to 2 and (g) mean size distribution of B1/DTPP 1 to 2.

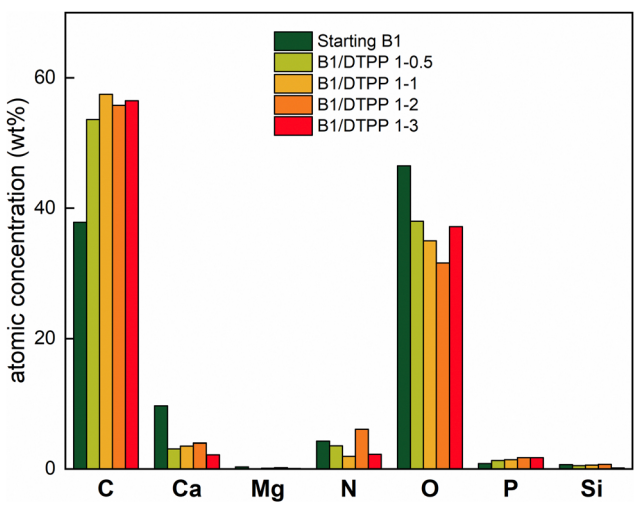

Fig. 5 Atomic distributions of elements for the tested specimens.

weight % rises to 1.74 corresponding to 13 wt% uptake. No further improvement was detected for B1/DTPP weight ratio of 1 to 3.

To have a quantitative evaluation of the DTPP uptake, an additional experiment of controlled pH release was performed on the B1/DTPP, being the EDX analysis limited to the powder surface. The release of DTPP was determined by UV measurements in the spectral range 200–350 nm on the aqueous solution at pH 1.3 (HCl 0.05 M).

As can be seen in Fig. 6d, the total ion release is completed after 5 h corresponding to 15 wt% uptake of DTPP. Conversely, in neutral conditions cation exchange is limited, resulting in only a negligible release (Fig. 6a) even after 7 hours. As a result of pH-sensitive cation release, the ionic nature of the product was verified, ruling out the possibility of sorption on the carbon matrix by secondary interactions as the mechanism responsible for the DTPP's uptake.

Therefore, a higher DTPP uptake can be obtained in the presence of the right salt excess providing a good degree of functionalization. DTPP amounts cannot exceed 15 wt%, which is the maximum possible uptake based on free OH groups.

To better optimize the process conditions, the chemical nature of the balls and the speed rate were changed. The reaction was performed in the presence of tempered steel (TS) and zirconia (ZrO_2) balls in the best reaction conditions previously defined (150 mg of a reagent mixture B1/DTPP in a ratio of 1 to 2 at 300 rpm).

As reported in Fig. 7, in all the cases the reaction takes place in 30 minutes as evident from the intense DTPP peaks present in the FTIR spectra. Interestingly, a slight reduction of the carbonyl peak at 1705 cm^{-1} appears evident for both milling treatments with tempered steel and zirconia balls.

Then, to deeply evaluate the real DTPP uptake after changing the chemical nature of the balls, additional experiments of controlled pH release were performed. As reported in Fig. 6, the total amount of DTPP in both the adducts coming from TS and

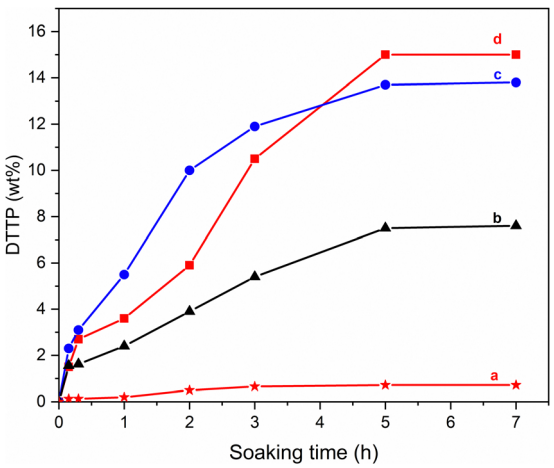

Fig. 6 DTPP release from B1/DTPP adduct: (a) obtained with silicon nitride (red curve, stars) in neutral solution, (b) tempered steel (blue curve, circles), (c) zirconia (black curve, triangles) and (d) Silicon nitride (red curve, squares), in acidic solution (pH = 1.3).

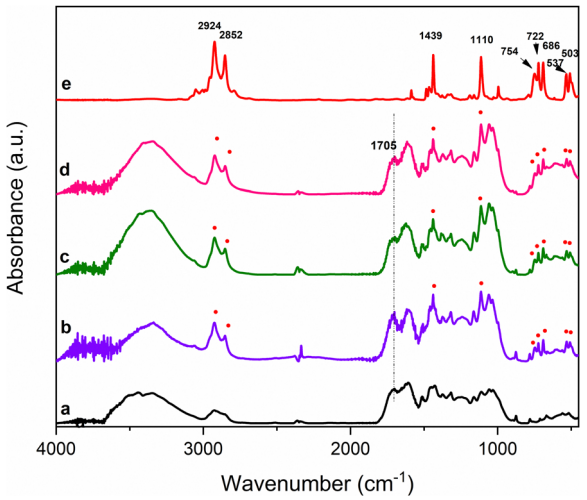

Fig. 7 FTIR spectra of: (a) B1, (b) B1/DTPP milled with silicon nitride, (c) tempered steel, (d) zirconia balls, and (e) DTPPBr.

ZrO_2 balls collisions, showed a comparable and reduced uptake, 14 wt% and 7.5 wt% respectively, as the comparison was done with silicon nitride.

Additionally, SEM/EDX analysis on the B1/DTPP adduct obtained by TS balls showed a consistent amount of iron released during the grinding. (see ESI†).

Further experiments were conducted to evaluate the effect of the speeding rate. The reaction was tested at 100 and 500 rpm by reducing and increasing the milling speed. Although the functionalization was not affected by increasing to 500 rpm, reducing to 100 rpm provided less DTPP uptake, requiring a longer time to reach the same degree of functionalization as previously reported.

By using the same functionalization procedure as B1 with B2, biochar from *Populous nigra* treated at 450 °C was used as a comparison study to investigate the role of oxygen functionalities on the carbon surface. The reaction was performed by using 200 mg of reagent mixture with B2/DTPP in a weight ratio of 1 to 2.

After recovering the powders, extensively washing with water, and drying at 60 °C, the B2/DTPP adduct was analyzed by FTIR spectroscopy. As clearly shown in Fig. 8, the peaks at 503, 537, 686, 722, 754, 1110, and 1439, cm^{-1} related to DTPP are missing, showing the inability of B2 to provide the adduct, due to the absence of the functional groups needed to promote the cation exchange.

Based on the research findings it has been determined that it is crucial to control the process temperature and keep it low to ensure that the appropriate oxygen functionalities, mainly hydroxyl groups, are present for promoting a fast cation exchange. Furthermore, as for the mechanochemical modification of the carbon black surface, ball milling should not restrict particular biochar to promote functionalization, as long as the necessary functional groups are present.

3.1 Dispersion test

The new modified carbon filler containing 15 wt% of DTPP can be suitable for antimicrobial properties, as previously reported

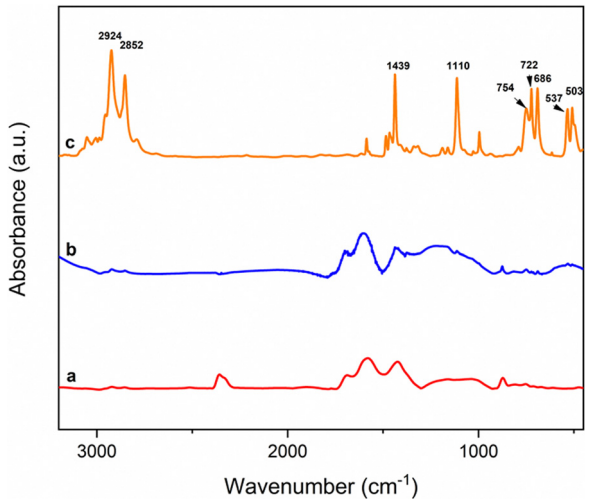

Fig. 8 FTIR spectra of (a) B2, (b) B2 after reaction with DTPP, and (c) DTPPBr.

for analogous QPS as clay,[28] graphite intercalated compounds[29] and MBQ.[30]

We tested the dispersion ability of B1/DTPP on a cotton fiber to prevent bacterial growth by using a coating process from an aqueous solution. The nanometric morphology associated with the chemical modification both obtained after grinding could ensure good interactions with the natural polymer matrix.

To this aim, cotton fabrics (150 $m^2\ g^{-1}$) were cut into square samples (2 cm × 2 cm) and were immersed in B1 and B1/DTPP aqueous solutions (2 wt%) under stirring. After 3 hours, the fabrics were taken out from the solutions and washed with distilled water to remove excess torrefied biomass from the surface. The obtained samples (named COTTON-B1 and COTTON-B1/DTPP) were allowed to dry at room temperature for 24 hours.

As reported in Fig. 9, pristine torrefied biomass seems not to be completely stuck on the cotton surface and is not homogeneously dispersed. Conversely, B1/DTPP, being nanometric and functionalized, appears to be uniformly dispersed on the cotton fabric as further confirmed by SEM images.

3.2 Photocatalytic activity

As antibacterial agents, inorganic nanoparticles like Ag, ZnO, and TiO_2[34,35] have been widely used to modify fabric surfaces, since they are capable of developing photocatalytic properties within textiles that can inhibit organic contamination and provide self-cleaning properties.

It was recently reported that cotton fabrics treated with GO have antibacterial activity against Gram-positive bacteria, proving that the surface modification of cotton fabrics with carbon powders might be an alternative to using inorganic particles.[36] The photocatalytic activity of GO-cotton fabrics has also been demonstrated by evaluating its ability to reduce resazurin (R) into resofurin (RF). Since the photocatalytic properties in textiles can be traced back to self-cleaning properties, this activity confirms the capacity to inhibit the growth of organic contaminants.

In order to evaluate the effect of the functionalization on torrefied biomass surface and the possible self-cleaning properties on the cotton fabrics, COTTON-B1 and COTTON-B1/DTPP prepared as described in the previous section, were subjected to photoreduction experiments under UV light.

Specifically, the phenoxazin-3-one dye, well-known as resazurin (R), was chosen as the reference substrate being a redox indicator used in many biological assays.[37] It shows intense and weak sorption at 602 nm and 380 nm due to π–π* transition of the phenoxazin-3-one and n–π* transition of the *N*-oxide, respectively. As a result of the reduction, *N*-oxide disappears and the conjugation changes, shifting maximum sorption to 572 nm.

The experiments were performed by immersing COTTON-B1 and COTTON-B1/DTPP in two separate resazurin aqueous solutions (1.5 μg ml^{-1}) and irradiating with a UV lamp at 350 nm. Absorption spectra were recorded at regular time intervals.

As reported in Fig. 10A, the presence of B1 in the cotton surface is not able to provide any conversion from R to RF even after 40 minutes, but only a slight decrease in the peak at 602 nm is observed probably due to simple adsorption of the

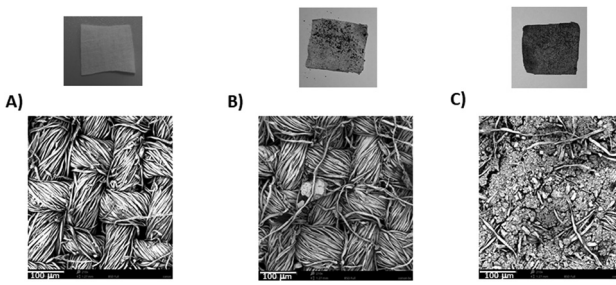

Fig. 9 Pictures and SEM images of (A) cotton fabric, (B) COTTON-B1, and (C) COTTON-B1/DTPP.

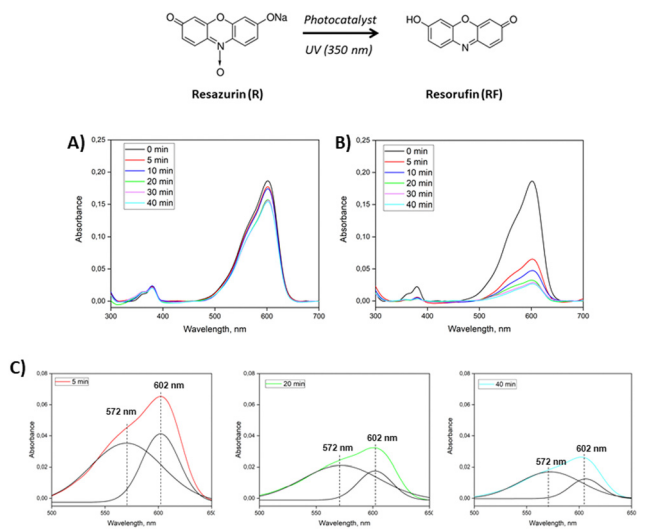

Fig. 10 Photocatalytic activity of COTTON-B1 (A) and COTTON-B1/DTPP (B) in resazurin aqueous solution under UV irradiation. (C) Deconvoluted spectra after 5, 20 and 40 min of reaction.

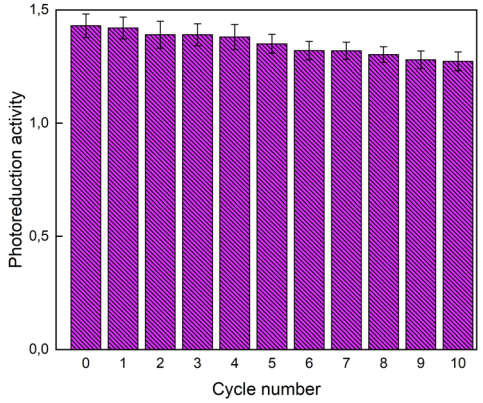

Fig. 11 Reusability tests of COTTON-B1/DTPP.

dye by the sample. Conversely, the presence of B1/DTPP (Fig. 10B) affords a sensible variation of the solution UV profile, with a substantial reduction of the 602 nm band intensity and the appearance of a pronounced shoulder centered at 572 nm as the photoreduction reaction proceeds.

In order to highlight the appearance of this new peak, the curves were analyzed by deconvolution. It is evident from the deconvoluted spectra that as the exposure time increases, the intensity of the peak at 572 nm increases (Fig. 10C). To confirm that the dye was reduced through the photocatalytic activity of the B1/DTPP and not simply adsorbed by the cotton, a further test was conducted without UV irradiation. In this case, there is a slight decrease in the peak at 602 nm (probably due to physical adsorption), and above all no appearance of the peak at 572 nm. (see ESI†). Moreover, a comparison with cotton modified with DTPPBr without biochar was reported to highlight the advantage of proposed functionalization. The results are summarized in Fig. S6 (ESI†). It is possible to observe that, since the low adhesion with cotton, the active DTPPBr didn't show any substantial activity. While, as reported previously, the DTPPBr functionalizated biochar allowed for obtaining a great photoreduction activity.

Finally, the COTTON-B1/DTPP sample, after the first photoreduction test, was rinsed with distilled water, dried and then subjected to an additional photoreduction test in order to verify the reusability of the produced system. This procedure was repeated 10 times and, for each cycle, the photoreduction activity was evaluated as the ratio of the absorbance of the peak at 572 nm to that of the peak at 602 nm. As shown in Fig. 11, system activity is preserved even after many cycles. In fact, a reduction of about 10% is observed after 10 cycles.

4 Conclusions

A green and sustainable functionalization of solid residue from *Populous nigra* treated at low pyrolysis temperature (T = 285 °C) with a mechanochemical approach without a precedent oxidation step has been reported, providing a new interesting filler with antimicrobial activity.

In a one-step procedure, the filler is nanometrically reduced and is properly functionalized *via* cation exchange in only 30 minutes in solvent-free conditions, providing a salt uptake of about 15 wt%. The product can be recovered without solvent assistance providing an environmentally friendly procedure.

Additionally, a comparative study using the biochar from populous nigra treated at 450 °C (B2) showed its inability to provide the adduct due to the absence of the functional groups needed to promote the cation exchange. This highlights the necessity to choose the right pyrolysis conditions to further functionalize the carbon surface. Only the low pyrolysis temperature ensures the presence of the appropriate oxygen functionalities to promote a fast cation exchange and prevent the additional oxidation step.

The nanometric morphology associated with the chemical modification both obtained after grinding, provides better dispersion ability on cotton fiber ensuring good interactions with the natural polymer matrix.

Finally, the antimicrobial properties of the new adduct have been demonstrated by measuring the photocatalytic activity of cotton fabrics coated with B1/DTPP adduct for the photoreduction of resazurin (R) into resorufin (RF) under UV light irradiation. The ability to develop photocatalytic properties within textiles can inhibit organic contamination and possibly provide self-cleaning properties.

The procedure is suitable for scale-up and the concepts developed in this work can be transferred to applied industrial chemistry.

Author contributions

M. R. A., G. G., A. K. contributed to the conception and design of the study, A. K. performed the experimental analysis, E. L., G. V. performed part of the characterization, M. R. A., P. G., C. M. G., R. R. wrote the first draft of the manuscript. All authors contributed to the manuscript revision, read, and approved the submitted version.

Conflicts of interest

There are no conflicts to declare.

Acknowledgements

This study was carried out within the Agritech National Research Center and received funding from the European Union Next-GenerationEU (PIANO NAZIONALE DI RIPRESA E RESILIENZA (PNRR) – MISSIONE 4 COMPONENTE 2, INVESTIMENTO 1.4 – D.D. 1032 17/06/2022, CN00000022). This manuscript reflects only the authors' views and opinions, neither the European Union nor the European Commission can be considered responsible for them. Prin 2022 PNRR ''DEveloping MEchanochemical Technologies to Render crop-protection Agrochemicals greener (DEMETRA)'' (contract number P202289FCM) is also gratefully acknowledged.

Notes and references

1 K. Weber and P. Quicker, Properties of Biochar, *Fuel*, 2018, **217**, 240.

2 C. M. Grottola, P. Giudicianni, S. Pindozzi, F. Stanzione, S. Faugno, M. Fagnano, N. Fiorentino and R. Ragucci, Steam Assisted Slow Pyrolysis of Contaminated Biomasses: Effect of Plant Parts and Process Temperature on Heavy Metals Fate, *Waste Manage.*, 2019, **85**, 232.

3 L. Liang, F. Xi, W. Tan, X. Meng, B. Hu and X. Wang, Review of Organic and Inorganic Pollutants Removal by Biochar and Biochar-Based Composites, *Biochar*, 2021, **33**, 255.

4 V. Dhyani and T. Bhaskar, A comprehensive review on the pyrolysis of lignocellulosic biomass, *Renewable Energy*, 2018, **129**, 695.

5 K. Weber and P. Quicker, Properties of biochar, *Fuel*, 2018, **217**, 240.

6 K. G. Kalogiannis, S. D. Stefanidis and A. A. Lappas, Ash Accumulation and Bio-Oil Deoxygenation during Ex Situ Catalytic Fast Pyrolysis of Biomass in a Cascade Thermal-Catalytic Reactor System, *Fuel Process. Technol.*, 2019, **186**, 99.

7 C. M. Grottola, P. Giudicianni, J. B. Michel and R. Ragucci, Torrefaction of Woody Waste for Use as Biofuel, *Energy Fuels*, 2018, **32**(10), 10266.

8 P. Giudicianni, V. Gargiulo, C. M. Grottola, M. Alfè, A. I. Ferreiro, M. A. Mendes, M. Fagnano and R. Ragucci, Inherent Metal Elements in Biomass Pyrolysis: A Review, *Energy Fuels*, 2021, **35**(7), 5407.

9 S. V. Vassilev, D. Baxter, L. K. Andersen and C. G. Vassileva, An Overview of the Chemical Composition of Biomass, *Fuel*, 2010, **89**(5), 913.

10 J. Lehmann and S. Joseph, Biochar for Environmental Management Science, Technology and Implementation, *Routledge, London, 2nd edn*, 2015.

11 J. H. Yuan, R. K. Xu and H. Zhang, The Forms of Alkalis in the Biochar Produced from Crop Residues at Different Temperatures, *Bioresour. Technol.*, 2011, **102**(3), 3488.

12 D. W. Rutherford, R. L. Wershaw and L. G. Cox, Changes in Composition and Porosity Occurring during the Thermal Degradation of Wood and Wood Components, *Scientific Investigations Report 2004-5292*, 2005.

13 P. Quicker and K. Weber, Biokohle: Herstellung, Eigenschaften Und Verwendung von Biomassekarbonisaten, Biokohle, *Springer Fachmedien, Wiesbaden*, 2016.

14 M. Bartoli, M. Troiano, P. Giudicianni, D. Amato, M. Giorcelli, R. Solimene and A. Tagliaferro, Effect of Heating Rate and Feedstock Nature on Electrical Conductivity of Biochar and Biochar-Based Composites, *Appl. Energy Combust. Sci.*, 2022, **12**, 100089.

15 S. Cheng, T. Chen, W. Xu, J. Huang, S. Jiang and B. Yan, Molecules Application Research of Biochar for the Remediation of Soil Heavy Metals Contamination: A Review, *Molecules*, 2020, **25**, 3167.

16 C. Abdy, Y. Zhang, J. Wang, Y. Yang, I. Artamendi and B. Allen, Pyrolysis of Polyolefin Plastic Waste and Potential Applications in Asphalt Road Construction: A Technical Review, *Resour., Conserv. Recycl.*, 2022, **180**, 106213.

17 E. S. Di Perta, P. Giudicianni, C. M. Grottola, A. Mautone, E. Cervelli, R. Ragucci and S. Pindozzi, Biochar Covering to Mitigate the Ammonia Emissions from the Manure Storage Tank: Effect of the Pyrolysis Temperature, *Metrol. Agric. For.*, 2022, 43.

18 C. Florio, P. Giudicianni, D. Pirozzi, V. Pasquale, R. Ragucci and S. Dumontet, Biochar as Improver of Methane Production in Anaerobic Digestion of Food Waste, *J. Environ. Acc. Manage.*, 2022, **8**(3), 267.

19 J. Wang and S. Wang, Preparation, Modification and Environmental Application of Biochar: A Review, *J. Cleaner Prod.*, 2019, **227**, 1002–1022.

20 M. Polok-Rubiniec and A. Włodarczyk-Fligier, Polypropylene Matrix Composite with Charcoal Filler, *J. Achiev. Mater. Manuf. Eng.*, 2020, **103**, 60.

21 J. Lewis, M. Miller, J. Crumb, M. Al-Sayaghi, C. Buelke, A. Tesser and A. Alshami, Biochar as filler in mixed matrix materials: Synthesis, characterization, and applications, *J. Appl. Polym.*, 2019, **136**(41), 48027.

22 M. Kumar, X. Xiong, Z. Wan, Y. Sun, D. C. W. Tsang, J. Gupta, B. Gao, X. Cao, J. Tang and J. Sik Ok, Ball milling as a mechanochemical technology for fabrication of novel biochar nanomaterials, *Bioresour. Technol.*, 2020, **312**, 123613.

23 C. Y. Liu and W. T. Cheng, Surface Modification and Characterization of Carbon Black through Oxidation, *Surf. Interface Anal.*, 2019, **51**(3), 316.

24 W. S. Hummers and R. E. Offeman, Preparation of Graphitic Oxide, *J. Am. Chem. Soc.*, 1958, **80**(6), 1339.

25 H. Liu, J. Wang, J. Wang and S. Cui, Sulfonitric Treatment of Multiwalled Carbon Nanotubes and Their Dispersibility in Water, *Materials*, 2018, **11**, 2442.

26 M. R. Acocella, M. Maggio, C. Ambrosio, N. Aprea and G. Guerra, Oxidized Carbon Black as an Activator of Transesterification Reactions under Solvent-Free Conditions, *ACS Omega*, 2017, **2**(11), 7862.

27 A. Kiani, N. Sozio and M. R. Acocella, Sustainable Functionalization of Carbon Black via Dry Ball Milling, *Mol. Syst. Des. Eng.*, 2023, **8**(7), 942.

28 L. Zhang, J. Chen, W. Yu, Q. Zhao and J. Liu, Antimicrobial Nanocomposites Prepared from Montmorillonite/Ag^{+}/Quaternary Ammonium Nitrate, *J. Nanomater.*, 2018, **2018**, 7.

29 A. G. Xie, X. Cai, M. S. Lin, T. Wu, X. J. Zhang, A. D. Lin and S. Tan, Long-acting antibacterial activity of quaternary phosphonium salts functionalized few-layered graphite, *Mater. Sci. Eng. B*, 2011, **176**, 1222.

30 Y. Fu, F. Wang, H. Sheng, M. Xu, Y. Liang, Y. Bian, S. A. Hashsham, X. Jiang and J. M. Tiedje, Enhanced Antibacterial Activity of Magnetic Biochar Conjugated Quaternary Phosphonium Salt, *Carbon*, 2020, **163**, 360.

31 T. Mahmood, M. T. Saddique, A. Naeem, P. Westerhoff, S. Mustafa and A. Alum, Comparison of Different Methods for the Point of Zero Charge Determination of NiO, *Ind. Eng. Chem. Res.*, 2011, **50**(17), 10017.

32 B. Chen, D. Zhou and L. Zhu, Transitional Adsorption and Partition of Nonpolar and Polar Aromatic Contaminants by Biochars of Pine Needles with Different Pyrolytic Temperatures, *Environ. Sci. Technol.*, 2008, **42**(14), 5137.
33 H. Yang, R. Yan, H. Chen, D. H. Lee and C. Zheng, Characteristics of Hemicellulose, Cellulose and Lignin Pyrolysis, *Fuel*, 2007, **86**(12–13), 1781.
34 G. Fu, P. S. Vary and C. T. Lin, Anatase TiO_2 Nanocomposites for Antimicrobial Coatings, *J. Phys. Chem.*, 2005, **109**(18), 8889.
35 B. Mahltig, F. Audenaert and H. Böttcher, Hydrophobic Silica Sol Coatings on Textiles-the Influence of Solvent and Sol Concentration, *J. Sol-Gel Sci. Technol.*, 2005, **34**(2), 103.
36 K. Krishnamoorthy, U. Navaneethaiyer, R. Mohan, J. Lee and S. J. Kim, Graphene Oxide Nanostructures Modified Multifunctional Cotton Fabrics, *Appl. Nanosci.*, 2012, **2**(2), 119.
37 C. Chakansin, J. Yostaworakul, C. Warin, K. Kulthong and S. Boonrungsiman, Resazurin Rapid Screening for Antibacterial Activities of Organic and Inorganic Nanoparticles: Potential, Limitations and Precautions, *Anal. Biochem.*, 2022, **637**, 114449.